AGU Advances

RESEARCH ARTICLE
10.1029/2020AV000273

This article is a companion to Repasch (2021), https://doi.org/10.1029/2021AV000402.

Key Points:

- Embankment and bank stabilization cuts off old floodplain organic carbon (OC) sources and expedites OC transmission in the Lower Mississippi River (LMR)
- Reduced river-floodplain exchange decreases the oxidative loss and increases the OC flux and export to the ocean by ≥ 40% in the LMR
- Embanking continental-scale rivers likely represents a significant change in global river-atmosphere-ocean carbon cycling

Supporting Information:

- Supporting Information S1
- Original Version of Manuscript
- Peer Review History
- Authors' Response to Peer Review Comments
- First Revision of Manuscript
- Second Revision of Manuscript
- Third Revision of Manuscript [Accepted]

Correspondence to:
Z. Shen,
zshen@coastal.edu

Citation:
Shen, Z., Rosenheim, B. E., Törnqvist, T. E., & Lang, A. (2021). Engineered continental-scale rivers can drive changes in the carbon cycle. *AGU Advances*, *2*, e2020AV000273. https://doi.org/10.1029/2020AV000273

Received 1 SEP 2020
Accepted 15 JAN 2021

Author Contributions:
Conceptualization: Zhixiong Shen, Brad E. Rosenheim, Torbjörn E. Törnqvist

Engineered Continental-Scale Rivers Can Drive Changes in the Carbon Cycle

Zhixiong Shen[1], Brad E. Rosenheim[2], Torbjörn E. Törnqvist[3], and Andreas Lang[4]

[1]Department of Marine Science, Coastal Carolina University, Conway, SC, USA, [2]College of Marine Science, University of South Florida, Saint Petersburg, FL, USA, [3]Department of Earth and Environmental Sciences, Tulane University, New Orleans, LA, USA, [4]Department of Geography and Geology, University of Salzburg, Salzburg, Austria

Abstract Floodplains of large alluvial rivers modulate the composition of riverine organic carbon (OC) and control OC oxidative loss, constituting a critical component in the global river-atmosphere-ocean carbon cycle. Therefore, anthropogenic management disconnecting rivers from their floodplains is expected to reduce the oxidative loss and to change the quality and quantity of riverine OC exported to the ocean. Here, we test this idea by combining two chronometers—^{14}C age spectra of OC and optically stimulated luminescence ages of quartz—to interrogate sediments of the Lower Mississippi River (LMR) system to constrain the anthropogenic effects on carbon cycling in a continental-scale sediment routing system. The ^{14}C age of the LMR OC has been reduced from >5,000 yr in prehistoric sediments to <3,000 yr in historic and modern sediments with significantly narrowed age spectrum width, following centuries of embanking the LMR. Bank stabilization reduced the river-floodplain sediment exchange by ~90%, effectively cutting off older floodplain OC from the river and reducing OC residence time in the severely truncated floodplain system, and expedited the downstream transmission of OC. The reduced residence time will have decreased riverine OC loss and enhanced younger OC delivery to marine sediments. We estimate that the oxidative loss of the LMR OC has been reduced by ≥ 1.1 Tg C/yr or 40%. Extrapolation to other large rivers that have undergone anthropogenic changes similar to the LMR illustrates that this process likely represents a carbon sink that can significantly increase if currently free-flowing large tropical rivers are embanked in the future.

Plain Language Summary Rivers play a key role in the global carbon cycle by releasing carbon dioxide to the atmosphere and controlling carbon transmission from land to ocean. How the carbon cycle has been affected by engineering activities that have fundamentally changed natural riverine processes is unclear. Using the Lower Mississippi River (LMR) as an example, we demonstrate that bank stabilization, which allows water and sediment to shoot through the river system directly into the ocean without interactions with the floodplain, can reduce river-floodplain organic carbon exchange by 90%. Consequently, carbon transport is expedited through such river systems, which decreases the amount of organic matter that is converted to CO_2 and, rather, increases its delivery to seafloor sediments. The loss of carbon from the LMR has been reduced by ≥ 40% or 1.1 Tg C per year due to river embankment, suggesting a significant human-caused shift in river-atmosphere-ocean carbon cycling that may occur in other large rivers as well.

1. Introduction

Rivers play an essential role in the global carbon cycle by exporting ~1 Pg C/yr (1 Pg = 10^{15} g) from land to ocean, outgassing ~1.1 Pg C/yr into the atmosphere, and storing ~0.6 Pg C/yr in lakes and reservoirs along their pathways in modern time (Aufdenkampe et al., 2011; Battin et al., 2009; Regnier et al., 2013; Tranvik et al., 2009). Organic carbon (OC) constitutes about half of the riverine carbon reaching the ocean as dissolved and particulate OC (DOC and POC, respectively). In ocean margins, POC dominates the buried terrestrial OC but with highly variable burial efficiency, ranging from <1% to nearly 100%, depending on its reactivity and integrated oxygen-exposure time, and broadly scaling with sediment accretion rate (Blair & Aller, 2012; Burdige, 2007). The burial of terrestrial OC in marine sediments is related primarily to sedimentation from large river systems (Burdige, 2005). River-ocean transfer of OC is a crucial process sequestering carbon from short-lived reservoirs, such as biomass and soils, into the reservoirs represented by marine sediments over geologic timescales (Berner, 1982).

Data curation: Zhixiong Shen, Brad E. Rosenheim, Torbjörn E. Törnqvist
Formal analysis: Zhixiong Shen, Brad E. Rosenheim, Andreas Lang
Funding acquisition: Zhixiong Shen, Brad E. Rosenheim, Torbjörn E. Törnqvist
Investigation: Zhixiong Shen, Brad E. Rosenheim, Torbjörn E. Törnqvist
Methodology: Zhixiong Shen, Brad E. Rosenheim, Torbjörn E. Törnqvist
Project Administration: Zhixiong Shen, Torbjörn E. Törnqvist
Resources: Brad E. Rosenheim, Andreas Lang
Supervision: Torbjörn E. Törnqvist
Writing – original draft: Zhixiong Shen
Writing – review & editing: Zhixiong Shen, Brad E. Rosenheim, Torbjörn E. Törnqvist, Andreas Lang

Riverine OC is a mixture of inputs from various sources that include highly refractory petrogenic carbon (OC_{petro}) that is devoid of ^{14}C and soil organic carbon (OC_{soil}) ranging in age from contemporary to thousands of years (Blair & Aller, 2012; Chaopricha & Marín-Spiotta, 2014). Small, mountainous rivers generally incorporate a bimodal distribution of contemporary OC_{soil} and OC_{petro} that is rapidly transported to the ocean (Blair & Aller, 2012; Milliman & Syvitski, 1992). In contrast, large, integrative river systems on passive margins can exhume large sources of aged OC_{soil} as they meander through expansive floodplains, allowing rivers to potentially liberate large quantities of OC locked away from the atmosphere for millennia. Floodplains in their pristine states affect river CO_2 outgassing (Scheingross et al., 2019) and regulate the composition of riverine OC exported to the ocean (Blair & Aller, 2012). However, the natural processes of OC exchange between rivers and floodplains and their effect on the carbon cycle remain poorly understood and mostly unaccounted for (Battin et al., 2009; Regnier et al., 2013), as is the role of interim OC storage in floodplains despite the large area they cover and the significant amounts of OC that are stored (Sutfin et al., 2016).

River systems have cradled human civilization for millennia and thus have been affected by prolonged anthropogenic activities, including land-use changes for agriculture (Klein Goldewijk et al., 2017) and, more recently, the accelerated introduction of river engineering through damming, embankment, and bank stabilization (Meybeck, 2003). These activities have changed the quantity of sediments routed to ocean margins (Syvitski et al., 2005), but understanding their impact on river-atmosphere-ocean carbon cycling remains a challenging issue (Bianchi & Allison, 2009). Agriculture-induced soil erosion increases the riverine OC flux (Regnier et al., 2013) and may have rendered this process a net carbon sink (S. V. Smith et al., 2001; Stallard, 1998; Van Oost et al., 2007). Damming alone has reduced the OC traveling through rivers to the oceans by ~13% due to burial and remineralization in reservoirs; this reduction is anticipated to approach 19% in the coming decade (Maavara et al., 2017). In large systems such as the Mississippi River, decreases in riverine OC transport due to land use and hydrographic changes have been observed (Bianchi et al., 2015). Furthermore, artificial levees and bank stabilization have largely disconnected the river from its floodplain (Meade & Moody, 2010). Overall, there is clear evidence that anthropogenic activities perturb riverine OC cycling. However, the effects of such changes on the composition, pathway, and cycling of riverine OC are not well quantified, even if conceptually expected to occur in altered river basins.

The apparent age distributions of OC, constrained by various separation methods of OC for radiocarbon dating in modern rivers, have been used to unravel the composition, sources, and transport pathways of OC (Alin et al., 2008; Galy et al., 2007; Goñi et al., 2014; Gordon & Goñi, 2003; Hedges et al., 1986; Hilton et al., 2015; Raymond & Bauer, 2001; Rosenheim & Galy, 2012; Rosenheim et al., 2013a; E. K. Williams et al., 2015). A recent study of a global data set of ~1,200 ^{14}C measurements revealed that the ages of present-day riverine OC range from modern to >20,000 ^{14}C yr (Marwick et al., 2015), demonstrating distinct spatial variability related to geologic (Leithold et al., 2006), hydrologic (Dalzell et al., 2007), climatic (Hilton et al., 2015), and anthropogenic (Longworth et al., 2007) controls. It has also been shown through compound-specific isotope methods that the ages and composition of OC vary temporally (Giosan et al., 2017; Schefuß et al., 2016).

In this study, we combine Ramped Pyrolysis Oxidation (RPO) ^{14}C analysis (Rosenheim et al., 2008) of OC with optically stimulated luminescence (OSL) dating of quartz grains to investigate independently dated ^{14}C age spectra of OC transmitted through the Lower Mississippi River (LMR) over the past ~1,000 years. Hence, we isolate temporal changes in the composition and pathway of OC in a continental-scale river system to elucidate the role of floodplains in carbon cycling, to examine the anthropogenic perturbations herein, and to discuss the significance of these findings for the global carbon cycle.

2. Study Area and Methods

2.1. The Mississippi River and Anthropogenic Changes

The Mississippi River drainage basin covers ~41% of the continental United States (Figure 1) and is mostly underlain by Phanerozoic sedimentary bedrock. The LMR runs through the ~30–100 km wide alluvial valley downstream of Cairo, Illinois (Figure 1), and receives its sediment and water inputs primarily from the Missouri and Ohio rivers, respectively (Meade & Moody, 2010). The bulk OC derived from the Missouri River mainly originates from erosion of grassland soils, whereas OC from the Ohio River consists mostly of woody materials (Bianchi, Wysocki, et al., 2007; Kendall et al., 2001). Migration and avulsion, the abrupt,

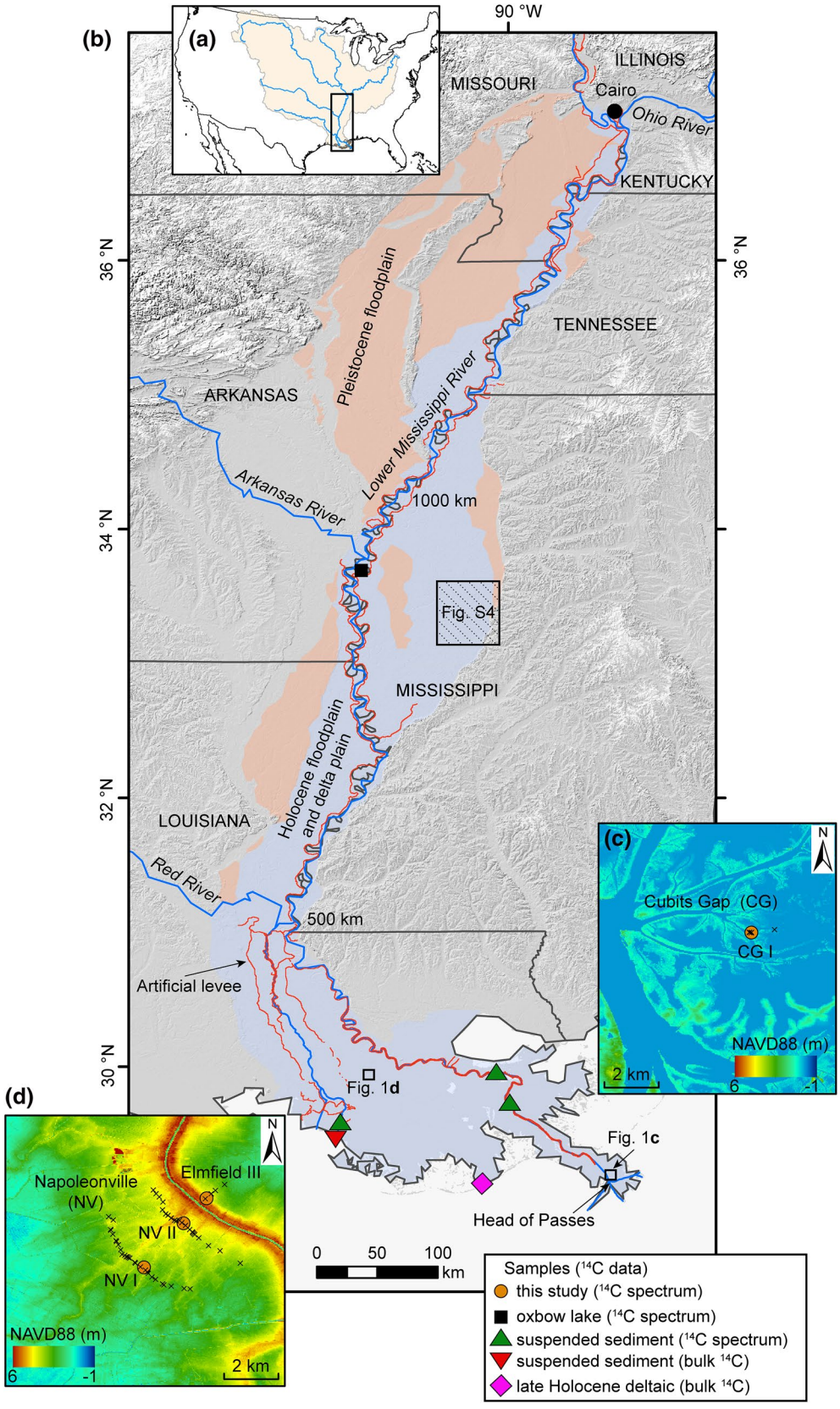
(a)
(b)
(c)
(d)
90 °W
36 °N
34 °N
32 °N
30 °N
ILLINOIS
MISSOURI
KENTUCKY
TENNESSEE
ARKANSAS
MISSISSIPPI
LOUISIANA
Cairo
Ohio River
Pleistocene floodplain
Lower Mississippi River
Arkansas River
Red River
Holocene floodplain and delta plain
1000 km
500 km
Fig. S4
Fig. 1d
Fig. 1c
Artificial levee
Head of Passes
0 50 100 km
Cubits Gap (CG)
CG I
NAVD88 (m)
6 -1
2 km
N
Napoleonville (NV)
Elmfield III
NV II
NV I
Samples (14C data)
this study (14C spectrum)
oxbow lake (14C spectrum)
suspended sediment (14C spectrum)
suspended sediment (bulk 14C)
late Holocene deltaic (bulk 14C)

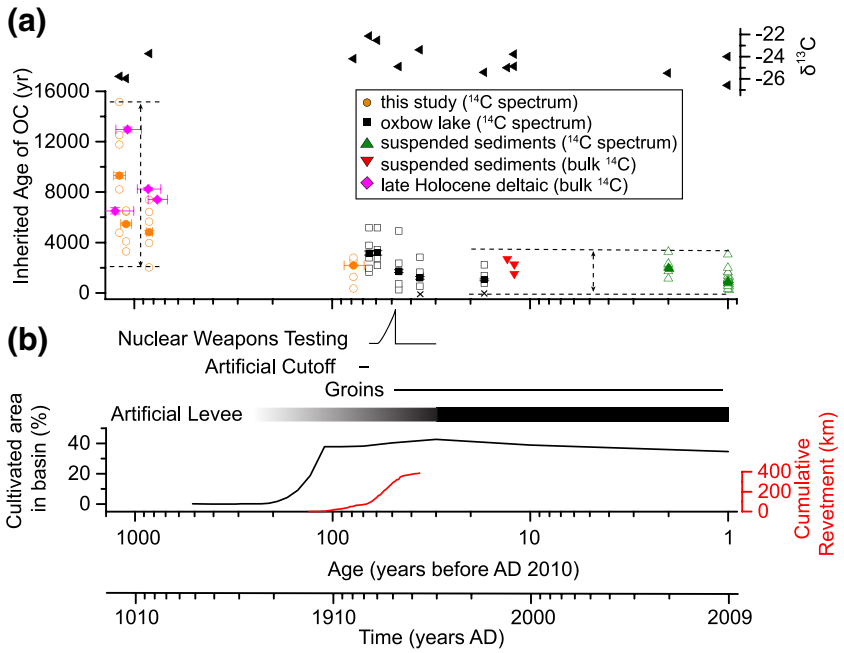

Figure 2. Inherited age of OC and major anthropogenic perturbations of the Lower Mississippi River. (a) Temporal evolution of OC mean inherited age (filled symbols), age spectra (open symbols), and $\delta^{13}C$ over the past millennium. The dashed lines and arrows sketch the maximum width of the age spectra of prehistoric and modern samples, respectively. Crosses indicate samples with ^{14}C ages younger than 1950 CE for which maximum inherited ages were used. Note that no $\delta^{13}C$ values from White (2017). (b) Nuclear weapons testing started in 1945, peaked in 1962, and ceased after 1980. History of major river engineering through artificial levees, cutoffs, groins, and bank revetments for a ~450 km segment between the confluences of the Arkansas and Red rivers (Meade & Moody, 2010; L. M. Smith & Winkley, 1996), and percentage of cultivated area within the Mississippi River drainage basin (Klein Goldewijk et al., 2017).

natural abandonment of an old river course for a new one, of the pristine LMR are mainly responsible for constructing its Holocene floodplain (Figure 1) (Saucier, 1994). The most downstream portion of the LMR resides in the Mississippi Delta that consists of five well-studied subdeltas formed by repeated avulsion of the lowermost LMR during the past ~6,000 years (Hijma et al., 2017).

Profound anthropogenic changes for agriculture, flood management, and river navigation have been made in the Mississippi River drainage basin during the past two centuries (Alexander et al., 2012; Harmar & Clifford, 2007; L. M. Smith & Winkley, 1996). The cultivated area expanded rapidly from ~1% of the drainage basin at the beginning of the 19th century to ~40% during the first half of the 20th century (Klein Goldewijk et al., 2017) (Figure 2), which resulted in a substantial increase in soil erosion during this period (Bennett & Chapline, 1928). Conversely, ensuing soil conservation practices drastically decreased erosion after the 1940s (Trimble, 1999). In the LMR, the change in the suspended sediment load related to the increase of soil erosion is not well quantified, but the load has been substantially reduced by damming. The construction of dams and reservoirs along tributaries of the LMR is mainly responsible for the decrease of its suspended sediment load from ~400–500 $\times 10^6$ t/yr before the 1950s to ~150 $\times 10^6$ t/yr today (Allison et al., 2000; Blum

Figure 1. The Lower Mississippi River (LMR) and its major geographic features. (a) The Mississippi River drainage basin. (b) The extent of Holocene and Pleistocene floodplains depicted after Saucier (1994); artificial levees are from the National Levee Database (http://nld.usace.army.mil/). Note that the artificial levees on both banks of the downstream portion of the LMR are located immediately adjacent to the channel. The oxbow lake samples are from Bianchi et al. (2015), the suspended sediment samples are from Rosenheim et al. (2013a) for ^{14}C spectra and Gordon and Goñi (2003) for bulk ^{14}C, and the late Holocene deltaic samples are from White (2017). For reference, river distance from Head of Passes is marked at multiple locations. (c and d) Digital elevation models of the Mississippi Delta study areas that contain (c) one historic sample and (d) three prehistoric samples. Crosses indicate core locations used to establish sedimentary architecture (Figure S1).

& Roberts, 2009; Meade & Moody, 2010; Sanks et al., 2020). Despite variability in sediment and soil delivery to the river, the LMR largely migrated naturally, exchanging sediments between the channel and floodplain during the early 20th century (Hudson & Kesel, 2000). However, the present-day LMR is constrained to an embanked floodplain ~5 km wide on average after centuries of engineering modifications (Figure 1). Artificial levees along the LMR were first constructed in the early 1700s and have grown higher and wider in a positive feedback loop with increasing flood magnitude (Munoz et al., 2018). Bank revetment by installing wooden or concrete erosion protections on the river-facing levee slope was introduced in the early 20th century to prevent bank caving and lateral migration of the LMR. The migration has been further constrained to maintain a stable navigation channel by a combination of dredging, cutoffs made in the 1930s to 1950s, and groins built after the 1950s (Meade & Moody, 2010; L. M. Smith & Winkley, 1996) (Figure 2).

2.2. Methods

OC age spectra of four late Holocene sediment samples from the Mississippi Delta were compared with historic to modern sedimentary OC to investigate the change of age spectra over the past ~1,000 years. The historic and modern OC data set consists of five sediment samples from an oxbow lake that was created in 1937 by a controlled neck cutoff of the LMR (Bianchi et al., 2015) and suspended sediments from near the mouth of the LMR (Rosenheim et al., 2013a) (Figure 1). Previously reported bulk ^{14}C ages of modern suspended sediments (Gordon & Goñi, 2003) and late Holocene deltaic sediments in the Mississippi Delta (White, 2017) (Figure 1, Text S1, Tables S1 and S2) were also included in this comparison.

The late Holocene sediment cores were taken from two study areas, Cubits Gap and Napoleonville (Figures 1c and 1d), both reported to have sediment accretion rates on the order of centimeters per year (Esposito et al., 2013; Shen et al., 2015). These cores sampled many of the clastic depositional settings of the Mississippi Delta, including mouth bar, natural levee, crevasse splay, and flood-basin. Rapid OC burial below the local groundwater table at these sites is expected to limit their postdepositional oxidative loss, including transformation of the ^{14}C age spectrum (Vetter et al., 2017). Thus, our focus on rapidly accreted deltaic deposits is vital because they likely most closely preserve the original ^{14}C age spectra at the time of deposition. OSL dating was used to measure the timing of deposition, and RPO ^{14}C analysis (Rosenheim et al., 2008) was used to determine the associated OC age spectra; the latter were subsequently used to calculate the weighted mean ^{14}C content of each sample (Rosenheim et al., 2013a, 2013b). The ^{14}C ages were calibrated with the IntCal20 calibration curve (Reimer et al., 2020) using the OxCal 4.4 program (Bronk Ramsey, 2009) prior to subtraction of the deposit ages to obtain inherited ages, that is, the age of OC at the time of deposition. Calibrated ^{14}C and OSL ages are reported with respect to 2010 CE.

To investigate the role of the floodplain in regulating OC composition and transmission pathways, as well as the anthropogenic impacts on these processes, we measured floodplain-to-river sediment fluxes for both the pristine and the embanked LMR.

2.2.1. Field Methods

The stratigraphy in the two study areas was investigated by means of sediment cores taken with a hand-operated Edelman auger and a gouge. An Eijkelkamp liner sampler, consisting of a metal cylinder and a plastic liner, was used for taking samples for OSL and RPO ^{14}C analysis (Shen et al., 2015). The Cubits Gap study area includes a historic bayhead delta (Figure 1c), and samples taken from very fine sandy facies interpreted as mouth-bar deposits (Figure S1) in two replicate cores at site CG I were used for OSL and RPO ^{14}C analysis, respectively. The Napoleonville study area (Figure 1d) features clayey to sandy facies interpreted as prehistoric overbank deposits representing natural-levee, crevasse-splay, and flood-basin deposits (Figure S1). Paired OSL and RPO ^{14}C analyses were performed at three sites (NV I, NV II, and EF III) in this area.

2.2.2. Optically Stimulated Luminescence Dating

The OSL samples were processed in a dark room to extract 4–11 μm (NV I-3a) or 75–125 μm (NV II-4a, EF III-1a, and CG I-1a) quartz grains (Table 1), following established procedures (Mauz et al., 2002). OSL dating instruments and the measurement protocol, data processing, and results were reported in an earlier

Table 1
OSL Dating Results

OSL sample[a]	Lab code	Sample depth (cm)	^{238}U (μg g^{-1})[b]	^{232}Th (μg g^{-1})	K_2O (μg g^{-1})	Water content	d_{cosmic} (Gy Kyr^{-1})[c]	Grain size (μm)[d]	n[e]	OD (%)[f]	De (Gy)	Age (yr)[g]
Cubits Gap I-1a	LV775	206–216	3.99 ± 0.08	9.77 ± 0.14	1.73 ± 0.05	0.32 ± 0.05	0.16	75–125	32	108	0.20 ± 0.02	78 ± 9
Napoleonville I-3a	LV639	420–435	4.04 ± 0.10	12.75 ± 0.27	2.20 ± 0.05	0.39 ± 0.05	0.11	4–11	12	4	2.31 ± 0.05	840 ± 30
Napoleonville II-4a	LV653	820–830	2.99 ± 0.08	8.48 ± 0.20	1.92 ± 0.05	0.27 ± 0.05	0.06	75–125	24	8	2.60 ± 0.08	1,100 ± 70
Elmfield III-1a	LV654	415–425	3.35 ± 0.09	10.56 ± 0.23	1.77 ± 0.05	0.24 ± 0.05	0.11	75–125	38	30	3.09 ± 0.11	1,190 ± 80

[a]Samples Napoleonville (NV) I-3a, II-4a, and Elmfield (EF) III-1a are from a previous publication (Shen et al., 2015). Note that paired OSL and RPO ^{14}C samples (Table 2) at each site are named with suffix a, b, c, d, e, and f, respectively. [b]Uncertainties are reported at the 1σ level throughout the table. [c]Cosmogenic dose rate. [d]Size of quartz grains used for OSL measurement. [e]Number of accepted aliquots included in the age calculation. [f]Overdispersion parameter characterizing the dispersion of measured dose distribution for a sample. [g]All results are reported as ages before 2010 CE.

study (Shen et al., 2015), except for the sample at the historic site (CG-1a). For CG I-1a, an early background subtraction technique (Chamberlain et al., 2018; Cunningham & Wallinga, 2010) (signal integrated over 0.64–1.76 s of an OSL decay curve serving as background) was used, whereas a late background subtraction (signal integrated over 32.16–40 s for background) was employed for the other three samples. The approach adopted for CG I-1a is based on a study indicating that early background subtraction results in higher accuracy for decadal-age samples from the Mississippi Delta (Shen & Mauz, 2012). Uncertainties in OSL dating originate from counting uncertainties of luminescence and gamma spectrometry measurements, water content variability of the deposits, and uncertainty in cosmic radiation received by the deposits. These uncertainties were accounted for following standard error propagation methods (Galbraith & Roberts, 2012; Shen et al., 2015).

2.2.3. Ramped Pyrolysis Oxidation ^{14}C Analysis

RPO ^{14}C analysis discretized ^{14}C of acid-insoluble OC according to the thermochemical stability of OC by pyrolyzing a sample to progressively higher temperature and rapidly oxidizing the pyrolysates to CO_2 for collection and analysis (Rosenheim et al., 2008). Recently biosynthesized OC tends to have lower thermochemical stability in comparison to aged OC. Therefore, this method is useful for investigating the composition and source of OC with mixed ages, typical of riverine OC (Rosenheim & Galy, 2012; Rosenheim et al., 2013a; E. K. Williams et al., 2015).

RPO ^{14}C samples were pretreated to remove carbonates with 1 N HCl for several hours and rinsed back to neutral pH with deionized water. Samples were then dried and pulverized. Aliquots of 100–400 mg, depending on the OC content of the sediment, were weighed into precombusted (525°C for 4 h) quartz reactors between precombusted (525°C for 4 h) layers of quartz wool. Reactor inserts were locked into the quartz pyrolysis/combustion reactors and heated at 5°C per minute from ambient temperature to 1000°C. Volatilized pyrolysis products were entrained in a He flow and transported into an oxidation reactor (with CuO, Ni, and Pt catalysts) at 800°C to produce CO_2, water, and other noncarbon bearing products of sequential pyrolysis/combustion at continuous temperature intervals. Subsequently, CO_2 was measured in an infrared gas analyzer and trapped for purification and quantification in a vacuum separations line and ultimately sealed into a borosilicate glass ampoule with copper oxide and silver wire for redundant combustion at 525°C for 2 h.

Samples were analyzed for ^{14}C content at the National Ocean Sciences Accelerator Mass Spectrometer (NOSAMS) facility at the Woods Hole Oceanographic Institution. The ^{14}C measurements were corrected for blank contamination related to the procedure of RPO preparation (Fernandez et al., 2014; Venturelli et al., 2020; Figure S2; Table S3). The analytical uncertainty of ^{14}C data was reported by NOSAMS (https://www.whoi.edu/nosams/radiocarbon-data-calculations) and standard error propagation was followed for processing the RPO ^{14}C data.

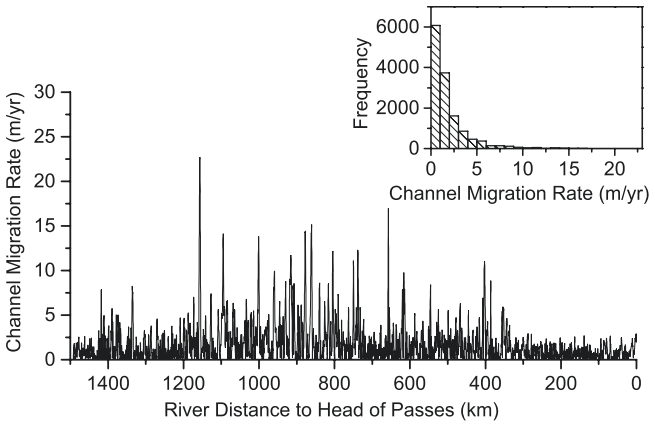

Figure 3. Lower Mississippi River channel mobility. Change in the position of the channel centerline was analyzed between the 1970s and 2019 using Landsat imagery available from the United States Geological Survey EarthExplorer (https://earthexplorer.usgs.gov/). The inset shows a histogram of all rates obtained.

2.2.4. Floodplain-to-River Sediment Flux

We investigated the sediment exchange between the river and floodplain when the LMR was "pristine" (prior to extensive river engineering) based on its lateral migration prior to the early 20th century. Hudson and Kesel (2000) calculated the maximum lateral migration rates during 1877–1924 for 125 meander bends of the LMR using two hydrographic surveys conducted by the Mississippi River Commission. The mean of the maximum rate (with a 95% confidence interval) was 38 ± 5 m/yr for the 825 km reach (L_1) between 1,055 and 1,880 river km from Head of Passes, and 59 ± 11 m/yr for the 410 km reach (L_2) between 645 and 1,055 river km from Head of Passes (river distance was measured along the LMR prior to the artificial cutoff that shortened the river. The 645, 1,055, and 1,880 pre-cutoff river km correspond to about 510, 830, and 1,485 river km from Head of Passes along the present LMR in Figure 1). Channel migration farther downstream was minimal due to the cohesive nature of prodelta clays comprising the banks and levees (Kolb, 1962), and therefore not considered here. Assuming that the maximum migration rate of a meander bend occurs at its apex and minimum migration at the inflection point, the mean migration rate along an individual meander bend is approximated by half of the apex value. Therefore, the mean lateral migration rate of the LMR was taken as 19 ± 3 m/yr (r_1) for segment L_1 and 30 ± 6 m/yr (r_2) for segment L_2. With a mean thalweg (the deepest part of the channel) depth with a 95% confidence interval being 26 ± 1 m (Figure S3), the sediment flux by bank caving due to migration of the pristine LMR (V_1) is calculated as:

$$V_1 = DL_1r_1 + DL_2r_2 \quad (1)$$

where L_1 and L_2 are the river lengths defined above, D is the mean thalweg depth, and r_1 and r_2 are the mean lateral migration rates indexed to the two river lengths defined above.

Landsat imagery taken in the 1970s and 2019 was obtained from the United States Geological Survey EarthExplorer (https://earthexplorer.usgs.gov/) and analyzed to quantify lateral migration of the embanked LMR (Text S2). The mean lateral migration rate of the LMR, with a 95% confidence interval, is 1.69 ± 0.03 m/yr during this time period (Figure 3). The volume of sediment produced by bank caving due to migration of the embanked LMR (V_2) is calculated as:

$$V_2 = DLr_3 \quad (2)$$

where L is the length of the 2019 LMR centerline (1,485 km), and r_3 is the mean lateral migration rate of the embanked LMR.

3. Age Spectra of Lower Mississippi River Organic Carbon

The three prehistoric samples at Napoleonville were OSL dated to 840 ± 30, 1,100 ± 70, and 1,190 ± 80 yr, respectively (Shen et al., 2015) (Table 1). Their mean OC ages are significantly older, ranging between 5,700 and 10,500 yr, corresponding to inherited mean ages (calibrated ^{14}C age minus OSL-derived depositional age) of 5,000–9,000 yr (Figure 2; Table 2). The mean OC ages correspond well to recently reported bulk ^{14}C ages of late Holocene Mississippi Delta sediments (White, 2017) (Figure 2). The age spectra of the prehistoric samples show a carbon pool with inherited ages >2,000 yr at the low-temperature end of OC pyrolysis and another pool with inherited ages of >6,500 yr at the high-temperature end. The sandy prehistoric sample has the oldest age spectrum with an inherited age >12,000 yr at the high-temperature end. The historic mouth-bar sand sample at Cubits Gap was OSL dated to 78 ± 9 yr and its OC has an inherited mean age of ~2,200 yr, that is, significantly younger than those of the prehistoric samples, but comparable to the inherited mean OC ages of independently dated LMR oxbow-lake deposits (Bianchi et al., 2015) as well as modern LMR sediments (Gordon & Goñi, 2003; Rosenheim et al., 2013a) (Figure 2). The age spectrum of

Table 2
Ramped Pyrolysis Oxidization (RPO) ^{14}C Dating Results

^{14}C sample[a]	OSL age (yr before 2010 CE)	Maximum pyrolysis T (°C)	Lab code (NOSAMS)	OC age (^{14}C yr BP)[b]	Calibrated OC age (yr before 2010 CE)[c]	Inherited OC age (yr)[b]	$\delta^{13}C$ (‰VPDB)
Cubits Gap I-1b	78 ± 9	345	OS-132456	310 ± 30	430 ± 60	350 ± 60	−25.12
Cubits Gap I-1c		381	OS-132457	1,380 ± 35	1,370 ± 30	1,290 ± 30	−23.58
Cubits Gap I-1d		419	OS-132458	2,480 ± 35	2,660 ± 105	2,580 ± 105	−23.23
Cubits Gap I-1e		499	OS-132459	2,740 ± 45	2,880 ± 50	2,805 ± 50	−24.58
Cubits Gap I-1f		695	OS-132460	6,050 ± 80	7,030 ± 180	6,950 ± 180	−24.60
				2,180 ± 20	**2,270 ± 90**	**2,195 ± 90**	**−24.22**
Napoleonville I-3b	840 ± 30	334	OS-107751	2,730 ± 50	2,875 ± 50	2,035 ± 55	−25.59
Napoleonville I-3c		406	OS-107737	4,240 ± 50	4,815 ± 105	3,975 ± 110	−23.97
Napoleonville I-3d		473	OS-107738	5,680 ± 70	6,505 ± 110	5,665 ± 115	−22.98
Napoleonville I-3e		578	OS-107739	6,310 ± 100	7,285 ± 190	6,445 ± 195	−23.43
Napoleonville I-3f		840	OS-108069	7,410 ± 240	8,255 ± 230	7,415 ± 230	−23.15
				4,860 ± 110	**5,660 ± 130**	**4,820 ± 130**	**−23.75**
Napoleonville II-4b	1,100 ± 70	307	OS-105660	3,910 ± 120	4,395 ± 185	3,295 ± 195	−27.51
Napoleonville II-4c		389	OS-105454	4,460 ± 45	5,190 ± 150	4,090 ± 165	−27.07
Napoleonville II-4d		436	OS-105551	6,650 ± 60	7,590 ± 50	6,490 ± 85	−25.00
Napoleonville II-4e		509	OS-105554	6,550 ± 60	7,550 ± 70	6,450 ± 100	−26.12
Napoleonville II-4f		735	OS-105661	6,730 ± 100	7,650 ± 85	6,550 ± 110	−25.05
				5,720 ± 80	**6,580 ± 110**	**5,480 ± 130**	**−25.98**
Elmfield III-1b	1,190 ± 80	349	OS-105662	5,150 ± 100	5,985 ± 180	4,795 ± 195	−26.88
Elmfield III-1c		409	OS-105663	8,370 ± 160	9,420 ± 170	8,230 ± 185	−25.29
Elmfield III-1d		456	OS-105664	11,770 ± 280	13,740 ± 335	12,550 ± 345	−25.88
Elmfield III-1e		562	OS-105665	10,980 ± 210	12,980 ± 165	11,790 ± 185	−26.04
Elmfield III-1f		801	OS-105994	13,490 ± 530	16,360 ± 770	15,170 ± 770	−24.70
				9,280 ± 160	**10,515 ± 205**	**9,325 ± 220**	**−25.79**

[a]Uncertainties are reported at the 1σ level throughout the table. Each sample was discretized to five ^{14}C samples of continuous temperature intervals by RPO. Note that paired OSL (Table 1) and discretized ^{14}C samples at each site are named with suffix a, b, c, d, e, and f, respectively. See Figure S2 for information about the correction of reported ^{14}C values for blank contamination during RPO preparation. [b]Bold numbers are ages calculated from weighted arithmetic means of ^{14}C content of discretized RPO samples. [c]The calibrated ^{14}C ages are reported as central value ± half range of the 1σ confidence interval of the calibrated ^{14}C data.

the historic sample shows a low-temperature carbon pool with an inherited age of ~350 yr (Figure 2), indicating a significant contribution of recent carbon fixation (Rosenheim et al., 2013a), and a high-temperature carbon pool with an inherited age of ~6,900 yr. Such a young low-temperature carbon pool is absent from the prehistoric samples, but persists in younger deposits, except for the two pre-1950 oxbow-lake deposits. In contrast, the high-temperature carbon pool is comparable in age to those of the prehistoric samples but not evident in the two youngest oxbow lake sediments or in the modern samples (Figure 2).

We reconstructed the change of the age spectra of OC transported through the LMR over the past ~1,000 years by comparing the new data presented here with the oxbow lake and modern river data (Bianchi et al., 2015; Rosenheim et al., 2013a). Over this period, both the mean inherited OC age and the width of the age spectrum show a marked decrease (Figure 2). The decrease is the result of the loss of a relatively refractory OC pool at the high-temperature end of OC pyrolysis with inherited ages >6,500 yr, and the enrichment of an OC pool at the low-temperature end of OC pyrolysis with inherited ages <1,000 yr. OC $\delta^{13}C$ values show little systematic variability and no temporal trend, consistent with mixing of OC sources with a distinct $\delta^{13}C$ signal in the LMR (Bianchi et al., 2015; Rosenheim et al., 2013a).

4. Discussion

4.1. Causes of Organic Carbon Change in the Lower Mississippi River

Compared to smaller, active margin river basins (Rosenheim & Galy, 2012), OC in the modern LMR system responds only subtly to changes in flow regime and changes in discharge source (Gordon & Goñi, 2003; Rosenheim et al., 2013a). The self-stabilizing behavior of large, passive-margin rivers can be expected due to the integrative nature of OC incorporation, storage, and transfer in vast floodplains (Blair & Aller, 2012; Rosenheim et al., 2013a). Over short timescales (storms and seasons) that mark carbon transport variability in small mountainous rivers (Milliman & Syvitski, 1992; Rosenheim & Galy, 2012), this represents a considerable stasis in carbon cycling of pristine passive margin rivers despite the changes in cross-sectional geometry, transport patterns, and disruption to floodplain ecology that mark high discharge events. On the other hand, large rivers have attracted concentrated human activity, including river engineering for flood control, agriculture, and other forms of water management. Thus, despite the pristine system stasis deriving from their large and integrative nature, large passive margin rivers are far from immune from the effects of human civilization over the last millennia, and especially the last century.

The organic matter associated with minerals of different size fractions may originate from diverse sources and often has varying ages (Alin et al., 2008; Bianchi, Galler, et al., 2007; Goñi et al., 2014; Gordon & Goñi, 2003). Therefore, composition and age variability of sedimentary OC in the Mississippi Delta may arise from hydraulic sorting during deposition. This is evidenced by the relatively large variability of the inherited ages, particularly at the high-temperature end of the age spectrum, among our three prehistoric samples and the four samples from White (2017) (Figure 2), as the texture of these samples varies from clay to sand. Nevertheless, the inherited ages of the prehistoric samples are all significantly older than the modern OC (Figure 2), suggesting that the decrease of the inherited OC age is independent of sediment type and location.

Engineering changes have caused local to regional bed degradation in the LMR and its tributaries. Dams constructed along the Missouri and Arkansas rivers during the 1950s and 1960s led to downstream bed degradation and bank erosion (G. P. Williams & Wolman, 1984). The artificial cutoffs in the 1930s to 1950s caused bed degradation in the middle part of the LMR (Harmar, 2004). Bank stabilization also prompted erosion of mid-Holocene peat beds and Pleistocene sediments in the lowermost reach of the LMR (Galler et al., 2003). Bed degradation is expected to release relatively old OC that would have increased the ^{14}C age of the modern LMR OC, which is not supported by our data (Figure 2). This suggests that the OC released by bed degradation is likely insignificant compared to the OC load of the LMR.

OC in the modern LMR is derived primarily from OC_{soil} in its drainage basin (Bianchi et al., 2015; Duan et al., 2007; Goñi et al., 1997; Gordon & Goñi, 2003; Onstad et al., 2000). Both topsoil erosion and gully erosion increased dramatically between the 1800s and 1940s due to the expansion of the cultivated area in the drainage basin (Bennett & Chapline, 1928). The eroded topsoil could be a major source of relatively young OC (up to a few thousand years old), whereas gully erosion also affects the subsoil and exports older OC_{soil} (Paul et al., 1997), as well as OC_{petro}. If these constituents were rapidly transmitted to the mouth of the LMR without major modification, we would expect the age of coeval LMR sedimentary OC to be older, with a wider spectrum than the prehistoric samples. However, the opposite is observed in the historic sample and the two oldest oxbow lake samples (Bianchi et al., 2015) representing this period. Furthermore, the inherited OC age spectrum does not show a distinct change corresponding to the drastic reduction in soil erosion after the 1940s (Bianchi et al., 2015). This suggests that changes in soil erosion were buffered by integration of the tributary systems of the LMR (Trimble, 1999).

Floodplains act as both sinks and sources of sediment and OC in naturally flooding and migrating alluvial rivers. Migration of the pristine LMR between 1877 and 1924 generated a floodplain-to-river sediment flux of $730 \pm 140 \times 10^6$ m^3/yr ($1{,}100 \pm 200 \times 10^6$ t/yr, assuming a bulk density of 1.5 t/m^3), closely matching an estimate made >100 years ago (Ockerson, 1892). Although deposition stored a similar amount of sediment back in the channel and floodplain (Kesel et al., 1992), mixing the sediment produced by bank caving with the 2–3 times smaller sediment flux from the Missouri River (Meade & Moody, 2010) made the floodplain-recycled material a major component of sediment and OC carried by the LMR to the ocean prior to 1950.

In contrast, analysis of Landsat imagery indicates that ~90% of the LMR has migrated <4 m/yr between the 1970s and 2019 (Figure 3). Erosion due to the migration of the entire LMR during this time interval generated a floodplain-to-river sediment flux of $72 \pm 4 \times 10^6$ m^3/yr ($110 \pm 6 \times 10^6$ t/yr). This represents a ~90% reduction in comparison to the period between 1877 and 1924. Even accounting for the reduction in suspended sediment load of the LMR due to damming, the 10-fold decrease in river-floodplain sediment exchange since the 1950s means that the contribution of recycled materials from the floodplain in the sediment load of the LMR has been dramatically reduced.

The LMR floodplain sediment contains OC with ages spanning the entire Holocene and even back into the last glacial. This is evident from the bulk ^{14}C ages of Holocene LMR channel-belt deposits that are as old as 20,000 yr (Saucier, 1983) (Figure S4 and Table S1). The floodplain has, to a large extent, been built by generations of meandering channel belts on top of late Pleistocene riverine sand and gravel (Saucier, 1994). A significant portion of the floodplain is occupied by flood basins that gradually accumulated sediment during most of the Holocene. The LMR in its natural state eroded into older channel belts and overbank strata, in addition to underlying deposits from the last glacial (Saucier, 1994) (Figure 1). This erosion reaches floodplain strata down to a depth equivalent to the thalweg depth, which differs from topsoil erosion in the hinterland that primarily mobilizes recently synthesized OC. Therefore, lateral migration of the pristine LMR could introduce abundant and significantly aged OC associated with both sand and mud that accounts for the high-temperature OC pool of the prehistoric sediments. We thus conclude that engineering modifications that reduced the river-floodplain sediment and OC exchange are the cause of the loss of the refractory pool of OC in the LMR.

The enrichment of the young OC pool is likely due to multiple causes. First, separating the LMR from its floodplain reduces temporary storage and speeds up the downstream transmission of sediment and OC so that the younger OC_{soil} from the hinterland can survive degradation and reach the river mouth.

Second, postdepositional remineralization may have preferentially removed young and more reactive OC in the prehistoric samples, even though the samples were taken deliberately from sediments that were buried rapidly below the local groundwater table. The thermographs of our four samples have similar shapes and maximum CO_2 evolution temperatures (T_{max}) (Figure S5), suggesting broadly comparable fractional remineralization. Riparian vegetation (Hupp et al., 2019) and instream algal production (Kendall et al., 2001) are sources of fresh and young OC for the LMR. The >2,000 yr inherited age for the youngest carbon pool suggests that the fresh OC is either insignificant or not efficiently buried and preserved in the prehistoric samples. However, thermographs of the oxbow-lake samples show a shoulder on the rising limb that is absent in our four samples, despite similar T_{max} (Bianchi et al., 2015), suggesting a higher contribution or better preservation of fresh OC in this depositional setting (Figure S5).

Third, damming of the Missouri and Arkansas rivers reduced the sediment load from these sources, which increased the relative proportion of the Ohio and Upper Mississippi river sediments (Meade & Moody, 2010) that carried relatively young, woody OC to the LMR (Bianchi et al., 2015). In addition, the post-1950 OC can be partly affected by anthropogenic ^{14}C from atmospheric testing of thermonuclear weapons, as previously demonstrated for the oxbow-lake sediments (Bianchi et al., 2015). However, these effects are not often observed unequivocally in modern age spectra or bulk ^{14}C ages from large, integrative river systems (Bouchez et al., 2010, 2014; Galy, Beyssac, et al., 2008; Hilton et al., 2015; Rosenheim et al., 2013a).

4.2. Floodplain Control of Riverine Organic Carbon

Blair and Aller (2012) proposed that floodplains of large passive-margin rivers modulate the composition of riverine OC through erosion-deposition cycles. The floodplain-river sediment exchange of the pristine LMR provides direct support for this model. Lateral migration of the pristine LMR resulted in a floodplain-to-river sediment flux of $1{,}100 \pm 200 \times 10^6$ t/yr. Assuming ~1% OC content, a conservative value for floodplain sediments (e.g., Aufdenkampe et al., 2011), the OC exchange between the LMR and its floodplain was 11 ± 2 Tg C/yr (1 Tg = 10^{12} g), which is 2–3 times the 4 Tg C/yr modern LMR OC flux to the ocean (Bianchi, Wysocki, et al., 2007).

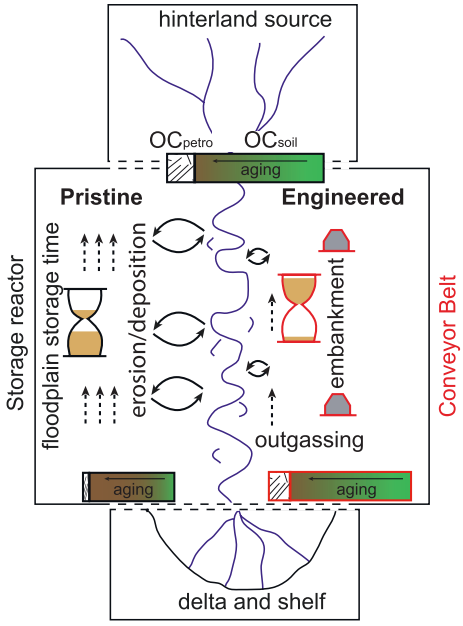

Figure 4. Contrasting floodplain control on riverine organic carbon (OC) between pristine and engineered rivers. The hinterland source feeds rivers with petrogenic carbon (OC_{petro}) and soil organic carbon (OC_{soil}). In the "storage reactor" model for pristine rivers, the floodplain and river exchange sediment and OC through erosion and deposition related to lateral migration and frequent flooding (Blair & Aller, 2012). Hinterland and riparian OC may be stored in floodplains for thousands of years, which results in aging of OC. OC is lost with CO_2 outgassing during floodplain storage, which may dominate riverine OC loss (Scheingross et al., 2019). OC_{petro} is depleted in the exported OC due to oxidation loss (Bouchez et al., 2010). In the "conveyor belt" model for engineered rivers, floodplain-river exchange is intercepted by embankment. As a result, hinterland source OC is transmitted through rivers with a short (if any) floodplain storage time and limited modifications.

The significantly aged OC exported by the prehistoric LMR (Figure 2) and other large pristine rivers (Goñi et al., 2014; E. K. Williams et al., 2015) indicates that floodplains of large rivers act as a "storage reactor" in modifying riverine OC (Figure 4). OC from hinterland sources and riparian vegetation can be stored for millennia in large floodplains. During storage, both OC_{petro} and OC_{soil} can be partly lost by oxidation and microbial respiration in favorable environments (Bouchez et al., 2010; Boye et al., 2017). The loss of OC_{petro} leads to the depletion of this component in the exported OC by large rivers, compared to small mountainous rivers (Blair & Aller, 2012). The oxidative loss of OC_{soil} preferentially removes the younger and more reactive constituent, although this loss can be partly compensated by OC synthesized by riparian vegetation (Goñi et al., 2014). Selective OC loss and the addition of riparian OC can also change $\delta^{13}C$ values of OC (Goñi et al., 2014; Gordon & Goñi, 2003). Oxidative loss during floodplain storage may dominate riverine CO_2 outgassing (Scheingross et al., 2019). Therefore, the floodplain "storage reactor" makes OC exported by large rivers compositionally different from OC derived from their hinterland sources.

The late Holocene to modern change of OC age spectra in the LMR suggest that the processes in the floodplain "storage reactor" have significantly subdued impacts on riverine OC when lateral channel migration is impeded by engineering modifications. An embanked river acts as a "conveyor belt" between the hinterland OC source and the marine sediment sink, largely bypassing the extensive floodplains (Figure 4). As a result, OC is transmitted through such rivers with truncated floodplain storage and limited modifications. The net result is that large integrative passive margin river systems such as the Mississippi River will approach the roles of small mountainous rivers on tectonically active margins which cycle carbon to the ocean more rapidly (Blair & Aller, 2012; Milliman & Syvitski, 1992), although small mountainous rivers contain a much larger proportion of OC_{petro} and tend to have higher OC burial efficiencies due to episodic high accretion rates and rapid burial in relatively deep water (Blair & Aller, 2012).

4.3. Implications for Cycling of Riverine Organic Carbon

Changing large OC routing systems from a "storage reactor" to a "conveyor belt" mode is likely to affect the river-atmosphere-ocean carbon cycle. Rivers can lose >50% of their POC load to the atmosphere during transit (Galy, France-Lanord, et al., 2008; Richey et al., 2002), and this loss may accrue predominantly by oxidation during floodplain storage (Scheingross et al., 2019). The DOC load probably exhibits even larger losses since it is more reactive (Marwick et al., 2015; Raymond & Bauer, 2001). Because OC oxidation depends on integrated oxygen-exposure time (Blair & Aller, 2012), reducing floodplain residence time by engineering could have reduced riverine OC loss, routing more OC to fluviodeltaic and offshore deposits. For a first-order constraint on the magnitude of the reduced OC loss, we assume that the pristine LMR lost ~50% of its OC load by oxidation during transit, which is likely a conservative value for rivers with large floodplains such as the Ganges (Galy et al., 2007) and the Amazon (Richey et al., 2002). Flume experiments showed that OC loss by fluvial transport up to ~1,000 km without floodplain storage is <10% (Scheingross et al., 2019; Zhao et al., 2020). If this applies to the LMR, its floodplain storage may account for at least 40% of the OC loss of the pristine LMR.

The mean inherited OC age is a maximum measure of the mean residence time of the LMR sediments in its floodplain and its value is at minimum ~5,000 yr for the pristine LMR and at maximum ~2,000 yr for the suspended sediment near the mouth of the modern LMR (Figure 2). Assuming oxidative loss of the whole

reactive floodplain OC pool, irrespective of OC age, follows the first-order single-pool decomposition model (Blair & Aller, 2012), the decrease of the reactive floodplain OC pool (C_r) with increasing floodplain storage duration (t) follows:

$$C_r \,/\, C_{r0} = e^{-kt} \tag{3}$$

where C_{r0} is the reactive OC pool at the time of floodplain deposition, and k is the decay constant. For the pristine LMR, the presumed ≥40% OC loss during a 5,000 yr floodplain storage produces a $k \geq 0.01\%$/yr. With this constraint on k, the oxidative loss of the OC load of the modern LMR is ≤ 20% for a floodplain storage duration ≤2,000 yr. Therefore, the shortened floodplain residence time reduces the presumed 40% OC load loss due to floodplain storage in the pristine LMR to ≤20%, which, in combination with the up to 10% riverine OC load loss by outgassing, suggests that the modern LMR probably loses ≤30% of its OC load. Based on the ≤30% OC load loss and the 4 Tg C/yr OC flux to the Gulf of Mexico of the modern LMR (Bianchi, Wysocki, et al., 2007), we estimate the maximum annual LMR OC load at 5.7 Tg C/yr. Assuming that the LMR OC load (excluding the fraction remineralized and buried behind dams) remains constant, the presumed 50% OC load loss of the pristine LMR equals ≤2.9 Tg C/yr. Therefore, the modern LMR OC flux to the Gulf of Mexico is ≥ 1.1 Tg C/yr, or 40%, larger than the pristine river (without accounting for the impact of dams) following embankment and bank stabilization.

The increased OC flux implies an increase of OC content in the exported sediment, concurring with the increase of both lignin and total OC concentration in post-1950 sediments in oxbow-lake deposits (Bianchi et al., 2015) and on the Louisiana continental shelf (Allison et al., 2007; Sampere et al., 2011). Our RPO ^{14}C analysis indicates that the LMR OC was rejuvenated because of losing the floodplain source of old OC. In addition, the sediment accretion rate on the Louisiana shelf has been reduced by 2–3 times due to the reduced sediment flux from the LMR since the 1950s (Allison et al., 2007). These changes may decrease the OC burial efficiency, which is, however, not supported by the lack of change in the OC remineralization rate in sediments on the Louisiana shelf with oxic bottom water (Allison et al., 2007). Therefore, we argue that the reduced OC loss by embanking the LMR leads to an increase of OC burial in marine sediments. This increases the continental shelf carbon sink fed by the LMR probably by ≥ 40%, even so the total sediment flux is reduced by damming.

It is well acknowledged that global riverine OC export to the oceans is strongly affected by anthropogenic modifications, including agriculture, urbanization, and damming (Maavara et al., 2017; Regnier et al., 2013), but the impact of bank stabilization has to date not been studied. Many large alluvial systems in densely populated regions have undergone anthropogenic changes similar to the LMR (Grill et al., 2019). Therefore, bank stabilization likely has increased global riverine OC export to the oceans and constituted a sink, considering the exceptionally constant OC burial efficiency in large river deltas (Blair & Aller, 2012). This sink may increase significantly if the still free-flowing major tropical rivers, including the Amazon, Congo (Schlünz & Schneider, 2000), and Ayeyarwady (Bird et al., 2008) that discharge a combined >10 times more OC than the LMR, were to be embanked in the future.

5. Conclusions

We combine RPO ^{14}C and OSL dating to unveil temporal changes in the ^{14}C age spectra of LMR OC over the past millennium. The ^{14}C age and age-spectrum width have been significantly reduced, independent of sediment type and location. This age reduction is ascribed primarily to the ~90% reduction in river-floodplain sediment exchange that cuts off the aged floodplain OC source, an unintended consequence of river engineering.

Floodplains play a critical role in controlling the OC flux in large pristine rivers. The floodplain acts as a "storage reactor" that mixes OC from various sources and stores it for thousands of years while preferentially remineralizing the younger and more reactive constituents. Sediment and OC exchange between floodplain and river can make floodplain-sourced, aged OC the dominant component exported by large rivers. However, when channel mobility is limited and lateral erosion hindered, sediment-routing systems are

disconnected from the floodplain reservoir and function as an efficient "conveyor belt" in the downstream transmission of hinterland OC.

We estimate that oxidative loss of OC transmitted through the LMR may have been reduced by at least 40% or 1.1 Tg C/yr due to the reduced storage time of OC in the floodplain. Because many large rivers have undergone or are undergoing intense modifications similar to the LMR, river engineering likely represents a significant shift in global river-atmosphere-ocean carbon cycling. We anticipate that additional studies of major rivers will allow for better constraints on the carbon cycling and coastal ocean biogeochemistry effects of increased worldwide river management.

Data Availability Statement

Data sets for this research including the OSL, ^{14}C data, and LMR channel centerlines and the 1973–2019 LMR migration rates are publicly available under Creative Commons Attribution 4.0 International (CC BY 4.0) license in Coastal Carolina University's Digital Common data repository (Shen et al., 2020). Data sets for this research are available in these in-text data citation references and repositories: The bulk ^{14}C data for late Holocene Mississippi Delta sediments from White (2017) (https://digitalcommons.lsu.edu/gradschool_dissertations/4100). The bulk ^{14}C data of Holocene LMR channel-belt deposits from Saucier (1983).

Acknowledgments
We thank E. L. Chamberlain, C. R. Esposito for field support, E. L. Chamberlain, S. Packman, M. Birchall, J. Tang for help in the laboratory, E. Wright for advice on channel-centerline analysis using ArcGIS, and M. A. Allison, and F. Peterse for discussions. The paper has been significantly improved after reviews by M. Repasch, S. Trumbore, and an anonymous reviewer. This project was supported by U.S. National Science Foundation grant EAR-1148005 to Shen, Törnqvist, and Rosenheim.

References

Alexander, J. S., Wilson, C. A., & Green, W. R. (2012). *A brief history and summary of the effects of river engineering and dams on the Mississippi River system and deltaRep*. U.S. Geological Survey Circular 1375, p. 43. Virginia: U.S. Geological Survey.

Alin, S. R., Aalto, R., Goñi, M. A., Richey, J. E., & Dietrich, W. E. (2008). Biogeochemical characterization of carbon sources in the Strickland and Fly rivers, Papua New Guinea. *Journal of Geophysical Research*, *113*, F01S05. https://doi.org/10.1029/2006jf000625

Allison, M. A., Bianchi, T. S., McKee, B. A., & Sampere, T. P. (2007). Carbon burial on river-dominated continental shelves: Impact of historical changes in sediment loading adjacent to the Mississippi River. *Geophysical Research Letters*, *34*, L01606. https://doi.org/10.1029/2006gl028362

Allison, M. A., Kineke, G. C., Gordon, E. S., & Goñi, M. A. (2000). Development and reworking of a seasonal flood deposit on the inner continental shelf off the Atchafalaya River. *Continental Shelf Research*, *20*(16), 2267–2294. https://doi.org/10.1016/S0278-4343(00)00070-4

Aufdenkampe, A. K., Mayorga, E., Raymond, P. A., Melack, J. M., Doney, S. C., Alin, S. R., et al. (2011). Riverine coupling of biogeochemical cycles between land, oceans, and atmosphere. *Frontiers in Ecology and the Environment*, *9*(1), 53–60. https://doi.org/10.1890/100014

Battin, T. J., Luyssaert, S., Kaplan, L. A., Aufdenkampe, A. K., Richter, A., & Tranvik, L. J. (2009). The boundless carbon cycle. *Nature Geoscience*, *2*(9), 598–600. https://doi.org/10.1038/Ngeo618

Bennett, H. H., & Chapline, W. R. (1928). *Soil erosion a national menace*Rep. United States Department of Agriculture Circular No. 33, p. 54. Washington, DC.

Berner, R. A. (1982). Burial of organic carbon and pyrite sulfur in the modern ocean: Its geochemical and environmental significance. *American Journal of Science*, *282*(4), 451–473. https://doi.org/10.2475/ajs.282.4.451

Bianchi, T. S., & Allison, M. A. (2009). Large-river delta-front estuaries as natural "recorders" of global environmental change. *Proceedings of the National Academy of Sciences of the United States of America*, *106*(20), 8085–8092. https://doi.org/10.1073/pnas.0812878106

Bianchi, T. S., Galler, J. J., & Allison, M. A. (2007), Hydrodynamic sorting and transport of terrestrially derived organic carbon in sediments of the Mississippi and Atchafalaya Rivers, *Estuarine Coastal and Shelf Science*, *73*(1–2), 211–222. https://doi.org/10.1016/j.ecss.2007.01.004

Bianchi, T. S., Galy, V., Rosenheim, B. E., Shields, M., Cui, X., & Van Metre, P. (2015). Paleoreconstruction of organic carbon inputs to an oxbow lake in the Mississippi River watershed: Effects of dam construction and land use change on regional inputs. *Geophysical Research Letters*, *42*(19), 7983–7991. https://doi.org/10.1002/2015gl065595

Bianchi, T. S., Wysocki, L. A., Stewart, M., Filley, T. R., & McKee, B. A. (2007). Temporal variability in terrestrially-derived sources of particulate organic carbon in the lower Mississippi River and its upper tributaries. *Geochimica et Cosmochimica Acta*, *71*(18), 4425–4437. https://doi.org/10.1016/j.gca.2007.07.011

Bird, M. I., Robinson, R. A. J., Win Oo, N., Maung Aye, M., Lu, X. X., Higgitt, D. L., et al. (2008). A preliminary estimate of organic carbon transport by the Ayeyarwady (Irrawaddy) and Thanlwin (Salween) Rivers of Myanmar. *Quaternary International*, *186*(1), 113–122. https://doi.org/10.1016/j.quaint.2007.08.003

Blair, N. E., & Aller, R. C. (2012). The fate of terrestrial organic carbon in the marine environment. *Annual Review of Marine Science*, *4*(1), 401–423. https://doi.org/10.1146/annurev-marine-120709-142717

Blum, M. D., & Roberts, H. H. (2009). Drowning of the Mississippi Delta due to insufficient sediment supply and global sea-level rise. *Nature Geoscience*, *2*, 488–491. https://doi.org/10.1038/ngeo553

Bouchez, J., Beyssac, O., Galy, V., Gaillardet, J., France-Lanord, C., Maurice, L., & Moreira-Turcq, P. (2010). Oxidation of petrogenic organic carbon in the Amazon floodplain as a source of atmospheric CO_2. *Geology*, *38*(3), 255–258. https://doi.org/10.1130/g30608.1

Bouchez, J., Galy, V., Hilton, R. G., Gaillardet, J., Moreira-Turcq, P., Pérez, M. A., et al. (2014). Source, transport and fluxes of Amazon River particulate organic carbon: Insights from river sediment depth-profiles. *Geochimica et Cosmochimica Acta*, *133*, 280–298. http://dx.doi.org/10.1016/j.gca.2014.02.032

Boye, K., Noël, V., Tfaily, M. M., Bone, S. E., Williams, K. H., Bargar, J. R., & Fendorf, S. (2017). Thermodynamically controlled preservation of organic carbon in floodplains. *Nature Geoscience*, *10*(6), 415–419. https://doi.org/10.1038/ngeo2940

Bronk Ramsey, C. (2009). Bayesian analysis of radiocarbon dates. *Radiocarbon*, *51*(1), 337–360. https://doi.org/10.1017/s0033822200033865

Burdige, D. J. (2005). Burial of terrestrial organic matter in marine sediments: A re-assessment. *Global Biogeochemical Cycles*, *19*, GB4011. https://doi.org/10.1029/2004gb002368

Burdige, D. J. (2007). Preservation of organic matter in marine sediments: Controls, mechanisms, and an imbalance in sediment organic carbon budgets? *Chemical Reviews*, *107*(2), 467–485. https://doi.org/10.1021/cr050347q

Chamberlain, E. L., Törnqvist, T. E., Shen, Z., Mauz, B., & Wallinga, J. (2018). Anatomy of Mississippi Delta growth and its implications for coastal restoration. *Science Advances*, *4*, eaar4740. https://doi.org/10.1126/sciadv.aar4740

Chaopricha, N. T., & Marín-Spiotta, E. (2014). Soil burial contributes to deep soil organic carbon storage. *Soil Biology and Biochemistry*, *69*, 251–264. https://doi.org/10.1016/j.soilbio.2013.11.011

Cunningham, A. C., & Wallinga, J. (2010). Selection of integration time intervals for quartz OSL decay curves. *Quaternary Geochronology*, *5*, 657–666.

Dalzell, B. J., Filley, T. R., & Harbor, J. M. (2007). The role of hydrology in annual organic carbon loads and terrestrial organic matter export from a midwestern agricultural watershed. *Geochimica et Cosmochimica Acta*, *71*(6), 1448–1462. http://dx.doi.org/10.1016/j.gca.2006.12.009

Duan, S., Bianchi, T. S., & Sampere, T. P. (2007). Temporal variability in the composition and abundance of terrestrially-derived dissolved organic matter in the lower Mississippi and Pearl Rivers. *Marine Chemistry*, *103*(1–2), 172–184. https://doi.org/10.1016/j.marchem.2006.07.003

Esposito, C. R., Georgiou, I. Y., & Kolker, A. S. (2013). Hydrodynamic and geomorphic controls on mouth bar evolution. *Geophysical Research Letters*, *40*(8), 1540–1545. https://doi.org/10.1002/grl.50333

Fernandez, A., Santos, G. M., Williams, E. K., Pendergraft, M. A., Vetter, L., & Rosenheim, B. E. (2014). Blank corrections for ramped pyrolysis radiocarbon dating of sedimentary and soil organic carbon. *Analytical Chemistry*, *86*(24), 12085–12092. https://doi.org/10.1021/ac502874j

Galbraith, R., & Roberts, R. G. (2012). Statistical aspects of equivalent dose and error calculation and display in OSL dating: An overview and some recommendations. *Quaternary Geochronology*, *11*, 1–27. https://doi.org/10.1016/j.quageo.2012.04.020

Galler, J. J., Bianchi, T. S., Allison, M., Wysocki, L. A., & Campanella, R. (2003). Biogeochemical implications of Levee Confinement in the lowermost Mississippi River. *Eos*, *84*, 469–470. https://doi.org/10.1029/2003EO440001

Galy, V., Beyssac, O., France-Lanord, C., & Eglinton, T. (2008). Recycling of graphite during Himalayan erosion: A geological stabilization of carbon in the crust. *Science*, *322*(5903), 943–945. https://doi.org/10.1126/science.1161408

Galy, V., France-Lanord, C., Beyssac, O., Faure, P., Kudrass, H., & Palhol, F. (2007). Efficient organic carbon burial in the Bengal fan sustained by the Himalayan erosional system. *Nature*, *450*(7168), 407–410. https://doi.org/10.1038/Nature06273

Galy, V., France-Lanord, C., & Lartiges, B. (2008). Loading and fate of particulate organic carbon from the Himalaya to the Ganga–Brahmaputra delta. *Geochimica et Cosmochimica Acta*, *72*(7), 1767–1787. https://doi.org/10.1016/j.gca.2008.01.027

Giosan, L., Ponton, C., Usman, M., Blusztajn, J., Fuller, D. Q., Galy, V., et al. (2017). Massive erosion in monsoonal central India linked to late Holocene land cover degradation. *Earth Surface Dynamics*, *5*(4), 781–789. https://doi.org/10.5194/esurf-5-781-2017

Goñi, M. A., Moore, E., Kurtz, A., Portier, E., Alleau, Y., & Merrell, D. (2014). Organic matter compositions and loadings in soils and sediments along the Fly River, Papua New Guinea. *Geochimica et Cosmochimica Acta*, *140*, 275–296. https://doi.org/10.1016/j.gca.2014.05.034

Goñi, M. A., Ruttenberg, K. C., & Eglinton, T. I. (1997). Source and contribution of terrigenous organic carbon to surface sediments in the Gulf of Mexico. *Nature*, *389*(6648), 275–278. https://doi.org/10.1038/38477

Gordon, E. S., & Goñi, M. A. (2003). Sources and distribution of terrigenous organic matter delivered by the Atchafalaya River to sediments in the northern Gulf of Mexico. *Geochimica et Cosmochimica Acta*, *67*(13), 2359–2375. https://doi.org/10.1016/S0016-7037(02)01412-6

Grill, G., Lehner, B., Thieme, M., Geenen, B., Tickner, D., Antonelli, F., et al. (2019). Mapping the world's free-flowing rivers. *Nature*, *569*(7755), 215–221. https://doi.org/10.1038/s41586-019-1111-9

Harmar, O. P. (2004). *Morphological and process dynamics of the lower Mississippi river* (Ph.D. Dissertation). Nottingham, UK: University of Nottingham.

Harmar, O. P., & Clifford, N. J. (2007). Geomorphological explanation of the long profile of the Lower Mississippi River. *Geomorphology*, *84*(3), 222–240. https://doi.org/10.1016/j.geomorph.2006.01.045

Hedges, J. I., Ertel, J. R., Quay, P. D., Grootes, P. M., Richey, J. E., Devol, A. H., et al. (1986). Organic carbon-14 in the Amazon River system. *Science*, *231*(4742), 1129–1131. https://doi.org/10.1126/science.231.4742.1129

Hijma, M. P., Shen, Z., Törnqvist, T. E., & Mauz, B. (2017). Late Holocene evolution of a coupled, mud-dominated delta plain–chenier plain system, coastal Louisiana, USA. *Earth Surface Dynamics*, *5*(4), 689–710. https://doi.org/10.5194/esurf-5-689-2017

Hilton, R. G., Galy, V., Gaillardet, J., Dellinger, M., Bryant, C., O'Regan, M., et al. (2015). Erosion of organic carbon in the Arctic as a geological carbon dioxide sink. *Nature*, *524*(7563), 84–87. https://doi.org/10.1038/nature14653

Hudson, P. F., & Kesel, R. H. (2000). Channel migration and meander-bend curvature in the lower Mississippi River prior to major human modification. *Geology*, *28*, 531–534. https://doi.org/10.1130/0091-7613(2000)28<531:cmamci>2.0.co;2

Hupp, C. R., Kroes, D. E., Noe, G. B., Schenk, E. R., & Day, R. H. (2019). Sediment trapping and carbon sequestration in floodplains of the lower Atchafalaya Basin, LA: Allochthonous versus autochthonous carbon sources. *Journal of Geophysical Research: Biogeosciences*, *124*(3), 663–677. https://doi.org/10.1029/2018jg004533

Kendall, C., Silva, S. R., & Kelly, V. J. (2001). Carbon and nitrogen isotopic compositions of particulate organic matter in four large river systems across the United States. *Hydrological Processes*, *15*(7), 1301–1346. https://doi.org/10.1002/hyp.216

Kesel, R. H., Yodis, E. G., & McCraw, D. J. (1992). An approximation of the sediment budget of the lower Mississippi River prior to major human modification. *Earth Surface Processes and Landforms*, *17*(7), 711–722. https://doi.org/10.1002/esp.3290170707

Klein Goldewijk, K., Beusen, A., Doelman, J., & Stehfest, E. (2017). Anthropogenic land use estimates for the Holocene – HYDE 3.2. *Earth System Science Data*, *9*, 927–953. https://doi.org/10.5194/essd-9-927-2017

Kolb, C. R. (1962). *Distribution and engineering significance of sediments bordering the Mississippi from Donaldsonville to the Gulf* (Ph.D. Dissertation). Baton Rouge, LA: Lousiana State University.

Leithold, E. L., Blair, N. E., & Perkey, D. W. (2006). Geomorphologic controls on the age of particulate organic carbon from small mountainous and upland rivers. *Global Biogeochemical Cycles*, *20*(3), GB3022. https://doi.org/10.1029/2005gb002677

Longworth, B. E., Petsch, S. T., Raymond, P. A., & Bauer, J. E. (2007). Linking lithology and land use to sources of dissolved and particulate organic matter in headwaters of a temperate, passive-margin river system. *Geochimica et Cosmochimica Acta*, *71*(17), 4233–4250. https://doi.org/10.1016/j.gca.2007.06.056

Maavara, T., Lauerwald, R., Regnier, P., & Van Cappellen, P. (2017). Global perturbation of organic carbon cycling by river damming. *Nature Communications*, *8*, 15347. https://doi.org/10.1038/ncomms15347

Marwick, T. R., Tamooh, F., Teodoru, C. R., Borges, A. V., Darchambeau, F., & Bouillon, S. (2015). The age of river-transported carbon: A global perspective. *Global Biogeochemical Cycles*, *29*(2), 122–137. https://doi.org/10.1002/2014gb004911

Mauz, B., Bode, T., Mainz, E., Blanchard, H., Hilger, W., Dikau, R., & Zöller, L. (2002). The luminescence dating laboratory at the University of Bonn: Equipment and procedures. *Ancient TL*, *20*, 53–61.

Meade, R. H., & Moody, J. A. (2010). Causes for the decline of suspended-sediment discharge in the Mississippi River system, 1940–2007. *Hydrological Processes*, *24*(1), 35–49. https://doi.org/10.1002/hyp.7477

Meybeck, M. (2003). Global analysis of river systems: From Earth system controls to Anthropocene syndromes. *Philosophical Transactions of The Royal Society B Biological Sciences*, *358*(1440), 1935–1955. https://doi.org/10.1098/rstb.2003.1379

Milliman, J. D., & Syvitski, J. P. M. (1992). Geomorphic/tectonic control of sediment discharge to the ocean: The importance of small mountainous rivers. *The Journal of Geology*, *100*, 525–544. https://doi.org/10.1086/629606

Munoz, S. E., Giosan, L., Therrell, M. D., Remo, J. W. F., Shen, Z., Sullivan, R. M., et al. (2018). Climatic control of Mississippi River flood hazard amplified by river engineering. *Nature*, *556*, 95–98. https://doi.org/10.1038/nature26145

Ockerson, J. A. (1892). *Caving banks from Cairo to Donaldsonville: 1877-83 to 1892*Rep. United States Mississippi river Commission Memphis, Tennessee.

Onstad, G. D., Canfield, D. E., Quay, P. D., & Hedges, J. I. (2000). Sources of particulate organic matter in rivers from the continental USA: Lignin phenol and stable carbon isotope compositions. *Geochimica et Cosmochimica Acta*, *64*(20), 3539–3546. https://doi.org/10.1016/S0016-7037(00)00451-8

Paul, E. A., Follett, R. F., Leavitt, S. W., Halvorson, A., Peterson, G. A., & Lyon, D. J. (1997). Radiocarbon dating for determination of soil organic matter pool sizes and dynamics. *Soil Science Society of America Journal*, *61*(4), 1058–1067. https://doi.org/10.2136/sssaj1997.03615995006100040011x

Raymond, P. A., & Bauer, J. E. (2001). Riverine export of aged terrestrial organic matter to the North Atlantic Ocean. *Nature*, *409*(6819), 497–500. https://doi.org/10.1038/35054034

Regnier, P., Friedlingstein, P., Ciais, P., Mackenzie, F. T., Gruber, N., Janssens, I. A., et al. (2013). Anthropogenic perturbation of the carbon fluxes from land to ocean. *Nature Geoscience*, *6*(8), 597–607. https://doi.org/10.1038/ngeo1830

Reimer, P. J., Austin, W. E. N., Bard, E., Bayliss, A., Blackwell, P. G., Bronk Ramsey, C., et al. (2020). The IntCal20 Northern Hemisphere radiocarbon age calibration curve (0–55 cal kBP). *Radiocarbon*, *62*, 1–33. https://doi.org/10.1017/rdc.2020.41

Richey, J. E., Melack, J. M., Aufdenkampe, A. K., Ballester, V. M., & Hess, L. L. (2002). Outgassing from Amazonian rivers and wetlands as a large tropical source of atmospheric CO_2. *Nature*, *416*(6881), 617–620. https://doi.org/10.1038/416617a

Rosenheim, B. E., Day, M. B., Domack, E., Schrum, H., Benthien, A., & Hayes, J. M. (2008). Antarctic sediment chronology by programmed-temperature pyrolysis: Methodology and data treatment. *Geochemistry, Geophysics, Geosystems*, *9*, Q04005. https://doi.org/10.1029/2007GC001816

Rosenheim, B. E., & Galy, V. (2012). Direct measurement of riverine particulate organic carbon age structure. *Geophysical Research Letters*, *39*(19), L19703. https://doi.org/10.1029/2012gl052883

Rosenheim, B. E., Roe, K. M., Roberts, B. J., Kolker, A. S., Allison, M. A., & Johannesson, K. H. (2013a). River discharge influences on particulate organic carbon age structure in the Mississippi/Atchafalaya River System. *Global Biogeochemical Cycles*, *27*(1), 154–166. https://doi.org/10.1002/gbc.20018

Rosenheim, B. E., Santoro, J. A., Gunter, M., & Domack, E. W. (2013b). Improving Antarctic sediment 14C dating using ramped pyrolysis: An example from the Hugo Island Trough. *Radiocarbon*, *55*(1), 115–126. https://doi.org/10.2458/azu_js_rc.v55i1.16234

Sampere, T. P., Bianchi, T. S., & Allison, M. A. (2011). Historical changes in terrestrially derived organic carbon inputs to Louisiana continental margin sediments over the past 150 years. *Journal of Geophysical Research*, *116*, G01016. https://doi.org/10.1029/2010JG001420

Sanks, K. M., Shaw, J. B., & Naithani, K. (2020). Field-based estimate of the sediment deficit in coastal Louisiana. *Journal of Geophysical Research: Earth Surface*, *125*, e2019JF005389. https://doi.org/10.1029/2019jf005389

Saucier, R. T. (1983). Geomorphological considerations related to cultural resources survey, Upper Yazoo Project, items 3 and 4. Appendix IV. In R. Thorne & H. K. Curry (Eds.), *Cultural resources survey of items 3 and 4, Upper Yazoo River projects, Mississippi, with a paleoenvironmental model of the Lower Yazoo Basin* (pp. 273–292). Mississippi: University of Mississippi.

Saucier, R. T. (1994). *Geomorphology and quaternary geologic history of the lower Mississippi valley*. Vicksburg: Mississippi River Commission.

Schefuß, E., Eglinton, T. I., Spencer-Jones, C. L., Rullkötter, J., De Pol-Holz, R., Talbot, H. M., et al. (2016). Hydrologic control of carbon cycling and aged carbon discharge in the Congo River basin. *Nature Geoscience*, *9*, 687. https://doi.org/10.1038/ngeo2778

Scheingross, J. S., Hovius, N., Dellinger, M., Hilton, R. G., Repasch, M., Sachse, D., et al. (2019). Preservation of organic carbon during active fluvial transport and particle abrasion. *Geology*, *47*(10), 958–962. https://doi.org/10.1130/g46442.1

Schlünz, B., & Schneider, R. R. (2000). Transport of terrestrial organic carbon to the oceans by rivers: Re-estimating flux- and burial rates. *International Journal of Earth Sciences*, *88*(4), 599–606. https://doi.org/10.1007/s005310050290

Shen, Z., & Mauz, B. (2012). Optical dating of young deltaic deposits on a decadal time scale. *Quaternary Geochronology*, *10*, 110–116. https://doi.org/10.1016/j.quageo.2012.01.014

Shen, Z., Rosenheim, B.E., Törnqvist, T. E., & Lang, A. (2020). *Anthropogenically expedited transit reduces organic carbon loss in the lower Mississippi river: Dataset*. Retrieved from https://digitalcommons.coastal.edu/science-data-sets/1/

Shen, Z., Törnqvist, T. E., Mauz, B., Chamberlain, E. L., Nijhuis, A. G., & Sandoval, L. (2015). Episodic overbank deposition as a dominant mechanism of floodplain and delta-plain aggradation. *Geology*, *43*(10), 875–878. https://doi.org/10.1130/g36847.1

Smith, L. M., & Winkley, B. R. (1996). The response of the Lower Mississippi River to river engineering. *Engineering Geology*, *45*(1), 433–455. http://dx.doi.org/10.1016/S0013-7952(96)00025-7

Smith, S. V., Renwick, W. H., Buddemeier, R. W., & Crossland, C. J. (2001). Budgets of soil erosion and deposition for sediments and sedimentary organic carbon across the conterminous United States. *Global Biogeochemical Cycles*, *15*(3), 697–707. https://doi.org/10.1029/2000GB001341

Stallard, R. F. (1998). Terrestrial sedimentation and the carbon cycle: Coupling weathering and erosion to carbon burial. *Global Biogeochemical Cycles*, *12*(2), 231–257. https://doi.org/10.1029/98GB00741

Sutfin, N. A., Wohl, E. E., & Dwire, K. A. (2016). Banking carbon: A review of organic carbon storage and physical factors influencing retention in floodplains and riparian ecosystems. *Earth Surface Processes and Landforms*, *41*(1), 38–60. https://doi.org/10.1002/esp.3857

Syvitski, J. P. M., Vörösmarty, C. J., Kettner, A. J., & Green, P. (2005). Impact of humans on the flux of terrestrial sediment to the global coastal ocean. *Science*, *308*, 376–380.

Tranvik, L. J., Downing, J. A., Cotner, J. B., Loiselle, S. A., Striegl, R. G., Ballatore, T. J., et al. (2009). Lakes and reservoirs as regulators of carbon cycling and climate. *Limnology and Oceanography*, *54*(6, Part 2), 2298–2314. https://doi.org/10.4319/lo.2009.54.6_part_2.2298

Trimble, S. W. (1999). Decreased rates of alluvial sediment storage in the Coon Creek Basin, Wisconsin, 1975-93. *Science*, *285*(5431), 1244. https://doi.org/10.1126/science.285.5431.1244

Van Oost, K., Quine, T. A., Govers, G., De Gryze, S., Six, J., Harden, J. W., et al. (2007). The impact of agricultural soil erosion on the global carbon cycle. *Science*, *318*(5850), 626–629. https://doi.org/10.1126/science.1145724

Venturelli, R. A., Siegfried, M. R., Roush, K. A., Li, W., Burnett, J., Zook, R., et al. (2020). Mid-Holocene grounding line retreat and readvance at Whillans Ice Stream, West Antarctica. *Geophysical Research Letters*, *47*(15), e2020GL088476. https://doi.org/10.1029/2020gl088476

Vetter, L., Rosenheim, B. E., Fernandez, A., & Törnqvist, T. E. (2017). Short organic carbon turnover time and narrow ^{14}C age spectra in early Holocene wetland paleosols. *Geochemistry, Geophysics, Geosystems*, *18*, 142–155. https://doi.org/10.1002/2016GC006526

White, C. M. (2017). *Influences of hurricanes, floods, and organic production on river-delta evolution over decadal to centennial timescales* (Ph.D. Dissertation). Baton Rouge, LA: Louisiana State University.

Williams, E. K., Rosenheim, B. E., Allison, M., McNichol, A. P., & Xu, L. (2015). Quantification of refractory organic material in Amazon mudbanks of the French Guiana Coast. *Marine Geology*, *363*, 93–101. https://doi.org/10.1016/j.margeo.2015.02.009

Williams, G. P., & Wolman, M. G. (1984). *Downstream effects of dams on alluvial rivers*. Washington, DC: Geological Survey Professional Paper 1286.

Zhao, M., Jacobs, L., Bouillon, S., & Govers, G. (2020). Soil organic carbon decomposition rates in river systems: Effect of experimental conditions. *Biogeosciences Discussions*, *2020*, 1–23. https://doi.org/10.5194/bg-2020-267

References From the Supporting Information

Alber, A., & Piégay, H. (2011). Spatial disaggregation and aggregation procedures for characterizing fluvial features at the network-scale: Application to the Rhône basin (France). *Geomorphology*, *125*(3), 343–360. https://doi.org/10.1016/j.geomorph.2010.09.009

Wolstencroft, M., Shen, Z., Törnqvist, T. E., Milne, G. A., & Kulp, M. (2014). Understanding subsidence in the Mississippi Delta region due to sediment, ice, and ocean loading: Insights from geophysical modeling. *Journal of Geophysical Research: Solid Earth*, *119*(4), 3838–3856. https://doi.org/10.1002/2013jb010928